EPJ Web of Conferences **20**, 02004 (2012)
DOI: 10.1051/epjconf/20122002004

Pseudoscalar Mesons Scattering off D^*-mesons with Chiral Perturbation Theory

Zhan-Wei Liu[1a], Yan-Rui Liu[2b], Xiang Liu[3c], and Shi-Lin Zhu[4d]

[1] Department of Physics and State Key Laboratory of Nuclear Physics and Technology
Peking University, Beijing 100871, China
[2] Department of Physics, H-27, Tokyo Institute of Technology, Meguro, Tokyo 152-8551, Japan
[3] School of Physical Science and Technology, Lanzhou University, Lanzhou 730000, China
[4] Department of Physics and State Key Laboratory of Nuclear Physics and Technology
and Center of High Energy Physics, Peking University, Beijing 100871, China

Abstract. We have systematically calculated the s-wave pseudoscalar mesons and D*-mesons scattering lengths to the third order with chiral perturbation theory, which will be helpful to reveal their strong interaction. We present the scattering lengths (1) in the framework of the heavy meson chiral perturbation theory and (2) in the framework of the infrared regularization.

1 Introduction

The hadron interaction is a hot topic in particle physics [1–8]. Scattering length is an important observable that contains the information of the hadron interaction. Low-energy hadron scattering involves the nonperturbative region of QCD.

Many new charmed particles have been discovered over the past few years. Some of them are speculated to be the candidates of the molecular states. The pseudoscalar meson and heavy vector D^*-meson might also form the molecular states if there exists strong attractive interaction between them.

Recently there have been some research papers devoted to the scattering of the pseudoscalar meson and heavy pseudoscalar D meson using different methods [9–11]. Here we will report the pseudoscalar meson and heavy vector D^*-meson scattering length with chiral perturbation theory.

Chiral perturbation theory is based on chiral symmetry and spontaneous chiral symmetry breaking. Its expansion parameter is the small momentum of the interacting particles. It is widely applied in many fields such as $\pi\pi$ scattering, $\gamma\gamma \to \pi\pi$, baryon form factors, πD scattering and so on. In this report we will use heavy meson effective field theory(HMEFT) [12–15] and infrared regularization method(IR)[16–19], which are both based on chiral perturbation theory, to study on pseudoscalar meson and D^* meson scattering.

We represent that the T-matrices of pseudoscalar meson and D^* meson scattering with HMEFT in Sec. 2. The T-matrices with IR are shown in Sec. 3 accompanied by the comparison of the two different methods. Then we will give a short summary in Sec. 4.

[a] Speaker, e-mail: liuzhanwei@pku.edu.cn
[b] e-mail: yrliu@th.phys.titech.ac.jp
[c] e-mail: xiangliu@lzu.edu.cn
[d] e-mail: zhusl@pku.edu.cn

2 The T-matrices with the Heavy Meson Chiral Perturbation Theory

Besides chiral symmetry we will also utilize the heavy quark symmetry which ensures that the system is independent on heavy quark spin and flavor. HMEFT has good power counting, that is the T-matrices at a certain order is only corresponding to definite relevant Feynman diagrams. We will calculate the πD^* s-wave scatting length to $O(\epsilon^3)$ at the threshold. For the calculations in detail, see the Ref. [20].

In the calculation we would use the following Lagrangians,

$$\mathcal{L}^{(2)}_{\phi\phi} = f^2 \mathrm{Tr}\left(u_\mu u^\mu + \frac{\chi_+}{4}\right), \tag{1}$$

$$\mathcal{L}^{(1)}_{H\phi} = -\langle (iv\cdot\partial H)\bar{H}\rangle + \langle Hv\cdot\Gamma\bar{H}\rangle + g\langle H \not{u}\gamma_5\bar{H}\rangle - \frac{1}{8}\delta\langle H\sigma^{\mu\nu}\bar{H}\sigma_{\mu\nu}\rangle, \tag{2}$$

$$\mathcal{L}^{(2)}_{H\phi} = c_0\langle H\bar{H}\rangle\mathrm{Tr}(\chi_+) + c_1\langle H\chi_+\bar{H}\rangle - c_2\langle H\bar{H}\rangle\mathrm{Tr}(v\cdot u\, v\cdot u) - c_3\langle Hv\cdot u\, v\cdot u\bar{H}\rangle, \tag{3}$$

$$\mathcal{L}^{(3)}_{H\phi} = \kappa_0\delta\langle H\bar{H}\rangle\mathrm{Tr}(\chi_+) + \kappa_1\delta\langle H\chi_+\bar{H}\rangle - \kappa_2\delta\langle H\bar{H}\rangle\mathrm{Tr}(v\cdot u\, v\cdot u) - \kappa_3\delta\langle Hv\cdot u\, v\cdot u\bar{H}\rangle + \kappa\langle H[\chi_-, v\cdot u]\bar{H}\rangle, \tag{4}$$

where H represents the lightest charmed doublet of D and D^* mesons, both u_μ and χ_- contain the odd numbers of Goldstone bosons, and Γ_μ contains even numbers of Goldstone bosons.

We would use the above Lagrangians to get the T-matrices. Loop-diagrams in Fig. 1 would generate the ultraviolet divergence in the terms containing L

$$L = \frac{\lambda^{D-4}}{16\pi^2}\left\{\frac{1}{D-4} + \frac{1}{2}(\gamma_E - 1 - \ln 4\pi)\right\}. \quad \text{(Euler constant } \gamma_E = 0.5772157) \tag{5}$$

But after wave function renormalization and the renormalization of the following low-energy constants

$$4\kappa_0 + \kappa_2 = \frac{2g^2L}{9f^2} + 4\kappa_0^r + \kappa_2^r, \quad \kappa_1 = \frac{5g^2L}{12f^2} + \kappa_1^r, \quad \kappa_3 = -\frac{3g^2L}{f^2} + \kappa_3^r, \quad \kappa = \frac{3L}{4f^2} + \kappa^r, \tag{6}$$

all infinities will be cancelled.

Then we will get

$$\begin{aligned} T^{(3/2)}_{\pi D^*} = & \left\{-\frac{m_\pi}{f_\pi^2}\right\} + \left\{\frac{(8c_0 + 4c_1 + 2c_2 + c_3)m_\pi^2}{f_\pi^2}\right\} + \left\{\frac{(8\kappa_0^r + 4\kappa_1^r + 2\kappa_2^r + \kappa_3^r)m_\pi^2\delta - 8m_\pi^3\kappa^r}{f_\pi^2}\right. \\ & \left. -\frac{1}{8}V(m_K, -m_\pi) - \frac{3}{8}V(m_\pi, -m_\pi) - \frac{1}{8}V(m_\pi, m_\pi) + \frac{1}{18}m_\pi^2 W(m_\eta) - \frac{1}{2}m_\pi^2 W(m_\pi) + 2V_1\right\} \\ & + \ldots, \end{aligned} \tag{7}$$

the terms in the first-, second- and third-bracket are at $O(\epsilon^1)$, $O(\epsilon^2)$ and $O(\epsilon^3)$ respectively. The superscript '3/2' of $T^{(3/2)}_{\pi D^*}$ in the bracket represents the total isospin of the channel. We find that $T^{(3/2)}_{\pi D^*}$ is equal to $T^{(3/2)}_{\pi D}$ in Ref. [9] when the mass difference δ between D and D^* approaches 0. There are 11 independent T-matrices in the pseudoscalar meson and D^* meson scattering due to the isospin symmetry, and the other 10 T-matrices are listed in Ref. [20].

To get the final numerical results we still need determine the low-energy constants, which can not be determined by chiral theory itself. Instead we can obtain them by fitting the experimental data. However, due to the lack of the relevant data, we resort to the resonance saturation model [21,22]. We consider the contribution of the $\sigma(600)$ singlet and $\kappa(800)$ octet as shown in Fig. 2(a), then integrate these intermediate particles, and finally get the relevant effective interacting vertices as in Fig. 2(b). Comparing the vertices with those in Lagrangian (3), one gets

$$c_0 = 0.031\ \mathrm{GeV}^{-1}, \quad c_1 = 0.12\ \mathrm{GeV}^{-1}, \quad c_2 = -0.024\ \mathrm{GeV}^{-1}, \quad c_3 = -0.091\ \mathrm{GeV}^{-1}. \tag{8}$$

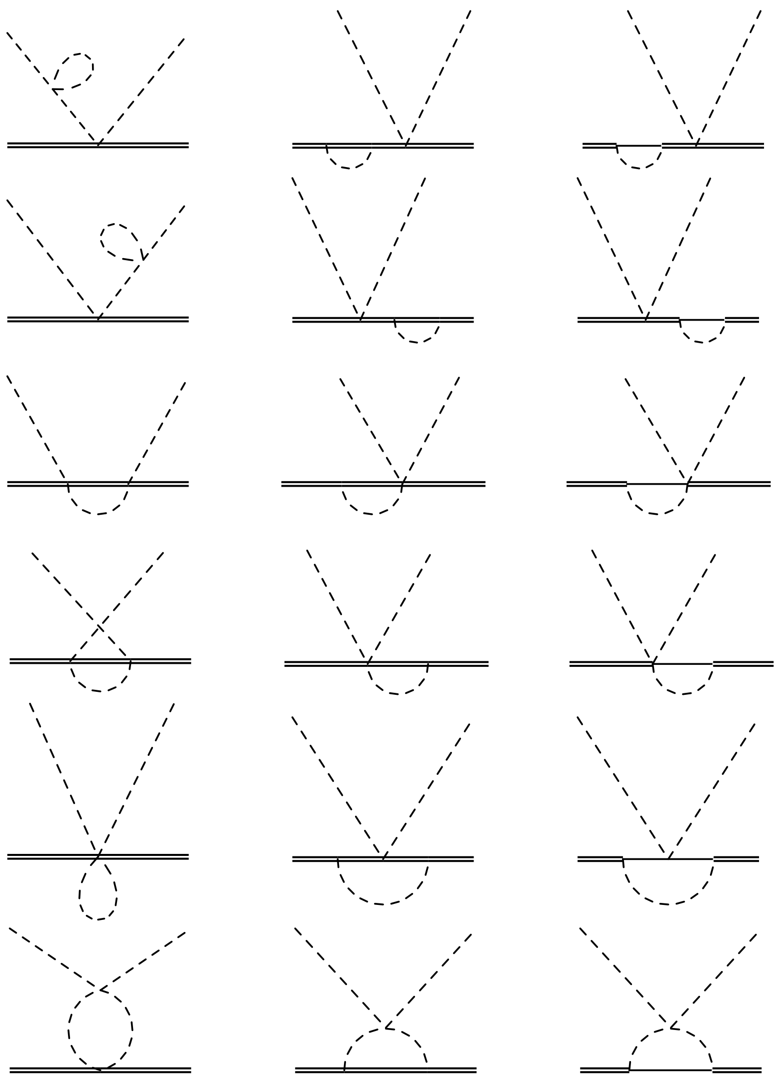

Fig. 1. Nonvanishing loop diagrams for the pseudoscalar meson and D^* meson scattering lengths to $O(\epsilon^3)$ with HMχPT and IR. The dashed lines, thin solid lines and thick solid lines represent the pseudoscalar Goldstone bosons, D mesons and D^* mesons, respectively.

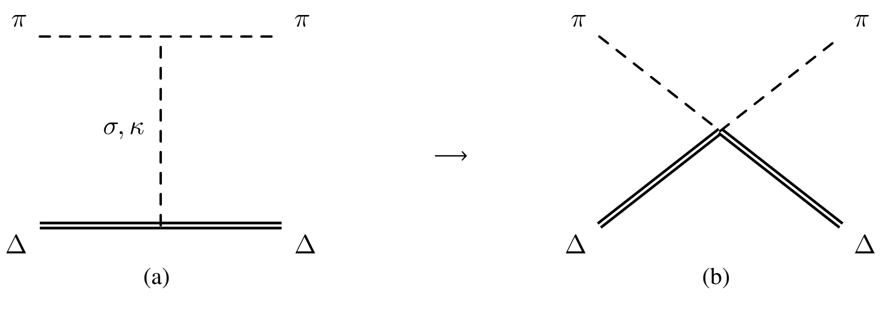

Fig. 2. Low-energy constants from the resonance saturation method

Table 1. The threshold T-matrices for the pseudoscalar meson and D^* meson scattering order by order in units of fm with HMχPT.

	$O(\epsilon^1)$	$O(\epsilon^2)$	$O(\epsilon^3)$			Total	Scattering length
			loop	tree	total		
$T^{(3/2)}_{\pi D^*}$	-3.2	0.27	-1.-0.0096i	0.17	-0.88-0.0096i	-3.8-0.0096i	-0.14-0.00036i
$T^{(1/2)}_{\pi D^*}$	6.5	0.27	0.53-0.0096i	-0.33	0.19-0.0096i	6.9-0.0096i	0.26-0.00036i
$T^{(1)}_{\pi D^*_s}$	0	0.09	-1.1	0	-1.1	-1.	-0.039
$T^{(0)}_{KD^*}$	15.	3.7	11.-0.00016i	-9.8	1.1-0.00016i	20.-0.00016i	0.64-5.2 $\times 10^{-6}i$
$T^{(1)}_{KD^*}$	0	0.75	-1.5+5.6i	0	-1.5+5.6i	-0.7+5.6i	-0.022+0.18i
$T^{(1/2)}_{KD^*_s}$	-7.6	2.2	-5.9	4.9	-0.98	-6.4	-0.21
$T^{(1)}_{\bar{K}D^*}$	-7.6	2.2	-7.4-0.000054i	4.9	-2.5-0.000054i	-7.9-0.000054i	-0.25-1.7 $\times 10^{-6}i$
$T^{(0)}_{\bar{K}D^*}$	7.6	-0.71	8.8+0.00016i	-4.9	3.9+0.00016i	11.+0.00016i	0.35+5.2 $\times 10^{-6}i$
$T^{(1/2)}_{\bar{K}D^*_s}$	7.6	2.2	4.+8.3i	-4.9	-0.86+8.3i	9.+8.3i	0.29+0.27i
$T^{(0)}_{\eta D^*}$	0	0.61	0.46+3.i	0	0.46+3.i	1.1+3.i	0.033+0.094i
$T^{(0)}_{\eta D^*_s}$	0	3.5	0.0036+6.1i	0	0.0036+6.1i	3.5+6.1i	0.11+0.19i

For the low-energy constants at the third order, the resonance saturation method would bring large uncertainty. So as in Ref. [9] we take

$$\kappa^r = -0.33 \text{ GeV}^{-2}, \tag{9}$$

which is obtained by fitting the data of the lattice calculation [23]. Other low-energy constants are just assumed to be negligible as done in Refs. [3,24].

We list the T-matrices of the πD^* scattering length in Table 1. We find that the chiral expansion of the pion-D^* channels converges well. The loop contribution in the kaon/eta-D^* channels is large due to the large mass of kaon/eta. Luckily it is cancelled mostly by the tree contribution at the same order, which makes the results at $O(\epsilon^3)$ smaller than that at the leading order as expected. The positive real part indicates that the strong interactions are attractive for the following channels: $a^{(1/2)}_{\pi D^*}$, $a^{(0)}_{KD^*}$, $a^{(0)}_{\bar{K}D^*}$, $a^{(1/2)}_{\bar{K}D^*_s}$, $a^{(0)}_{\eta D^*}$ and $a^{(0)}_{\eta D^*_s}$.

3 The T-matrices with the Infrared Regularization Method

IR has both good power counting and correct analyticity since IR formalism includes the higher-order infrared parts of the loop graphs. Relativistic Lagrangians will be used in IR. When calculating loop integral $\int d^dk$, the integral is replaced by the infrared integral $\int_I d^dk$. The replacement would drop some terms. But the dropped terms could be absorbed by tree diagrams. Thus it is just a redefinition of low-energy constants.

IR was first introduced to study the πN scattering [16]. Here we extend it to study the πD^* scattering. We obtain the T-matrices with the following relativistic Lagrangians,

$$\begin{aligned}
\mathcal{L}^{(1)}_{H\phi} &= \mathcal{D}_\mu \tilde{P} \mathcal{D}^\mu \tilde{P}^\dagger - \mathring{M}^2 \tilde{P}\tilde{P}^\dagger - \mathcal{D}_\mu \tilde{P}^{*\nu} \mathcal{D}^\mu \tilde{P}^{*\dagger}_\nu + (\mathring{M}+\delta)^2 \tilde{P}^{*\nu}\tilde{P}^{*\dagger}_\nu \\
&\quad + i2g\mathring{M}(\tilde{P}^*_\mu u^\mu \tilde{P}^\dagger - \tilde{P} u^\mu \tilde{P}^{*\dagger}_\mu) + g(\tilde{P}^*_\mu u_\alpha \mathcal{D}_\beta \tilde{P}^{*\dagger}_\nu - \mathcal{D}_\beta \tilde{P}^*_\mu u_\alpha \tilde{P}^{*\dagger}_\nu)\epsilon^{\mu\nu\alpha\beta}, && (10)\\
\mathcal{L}^{(2)}_{H\phi} &= 2\mathring{M}(c_0 \tilde{P}^{*\mu}\tilde{P}^{*\dagger}_\mu \mathrm{Tr}(\chi_+) + c_1 \tilde{P}^{*\mu}\chi_+\tilde{P}^{*\dagger}_\mu - c_2 \tilde{P}^{*\mu}\tilde{P}^{*\dagger}_\mu \mathrm{Tr}(u\cdot u) - c_3 \tilde{P}^{*\mu} u\cdot u\tilde{P}^{*\dagger}_\mu), && (11)\\
\mathcal{L}^{(3)}_{H\phi} &= 2\mathring{M}(\kappa_0 \tilde{P}^{*\mu}\tilde{P}^{*\dagger}_\mu \mathrm{Tr}(\chi_+)\delta + \kappa_1 \tilde{P}^{*\mu}\chi_+\tilde{P}^{*\dagger}_\mu\delta - \kappa_2 \tilde{P}^{*\mu}\tilde{P}^{*\dagger}_\mu \mathrm{Tr}(u\cdot u)\delta - \kappa_3 \tilde{P}^{*\mu} u\cdot u\tilde{P}^{*\dagger}_\mu\delta) \\
&\quad + i\mathring{M}\kappa\left(\mathcal{D}_\nu \tilde{P}^{*\mu}[\chi_-, u^\nu]\tilde{P}^{*\dagger}_\mu - \tilde{P}^{*\mu}[\chi_-, u^\nu]\mathcal{D}_\nu \tilde{P}^{*\dagger}_\mu\right), && (12)
\end{aligned}$$

where

$$\tilde{P} = \frac{P}{\sqrt{\mathring{M}}}, \quad \mathcal{D}_\mu \tilde{P}_a = \partial_\mu \tilde{P}_a - \Gamma^{ba}_\mu \tilde{P}_b, \quad \mathcal{D}_\mu \tilde{P}^\dagger_a = \partial_\mu \tilde{P}^\dagger_a + \Gamma^{ab}_\mu \tilde{P}^\dagger_b. \qquad \text{(Similar for } \tilde{P}^*.) \tag{13}$$

Table 2. Comparison of the T-matrices from the loop diagrams for the pseudoscalar meson and D^* meson scattering between HMχPT and IR.

	Intermediate state: D meson		Intermediate state: D^* meson		Loop: total	
	HMχPT	IR	HMχPT	IR	HMχPT	IR
$T^{(3/2)}_{\pi D^*}$	-0.053-0.0096i	-0.043-0.0076i	-0.99	-0.84	-1.-0.0096i	-0.88-0.0076i
$T^{(1/2)}_{\pi D^*}$	-0.053-0.0096i	-0.05-0.0093i	0.58	0.3	0.53-0.0096i	0.25-0.0093i
$T^{(1)}_{\pi D^*_s}$	-0.043	-0.03	-1.1	-0.88	-1.1	-0.91
$T^{(0)}_{KD^*}$	0.69-0.00016i	0.46-0.00015i	10.	7.5	11.-0.00016i	8.-0.00015i
$T^{(1)}_{KD^*}$	-0.076+0.000054i	-0.014+0.0019i	-1.4+5.6i	-3.6+2.9i	-1.5+5.6i	-3.6+2.9i
$T^{(1/2)}_{KD^*_s}$	0.46	0.29	-6.3	-13.	-5.9	-13.
$T^{(1)}_{\bar{K}D^*}$	0.31-0.000054i	0.17-0.00099i	-7.7	-14.	-7.4-0.000054i	-14.-0.00099i
$T^{(0)}_{\bar{K}D^*}$	-0.46+0.00016i	-0.33-0.0027i	9.3	11.	8.8+0.00016i	11.-0.0027i
$T^{(1/2)}_{\bar{K}D^*_s}$	0.46	0.31	3.6+8.3i	1.1+4.4i	4.+8.3i	1.5+4.4i
$T^{(0)}_{\eta D^*}$	0.14+0.0021i	0.088+0.0018i	0.32+3.i	-2.9+1.6i	0.46+3.i	-2.8+1.6i
$T^{(0)}_{\eta D^*_s}$	-0.022	-0.015	0.025+6.1i	-6.2+3.2i	0.0036+6.1i	-6.2+3.2i

If letting the heavy meson mass approach infinity, we verify that the results with IR are the same with those with HMEFT. The difference between IR and HMEFT results from the different loop integrals. So here we only list the numerical comparison of the loop diagrams in Table 2. From Table 2, one can see that the difference is not very large in the numerical results between the two methods. Also we find that the contribution with the intermediate D^* meson dominates the loop contribution in both cases of HMEFT and IR. The difference is not very large in the numerical results between the two methods.

4 Summary

In short summary, we have calculated the pseudoscalar meson and heavy vector meson scattering length to the third order. We found there exists attractive interaction in some channels, which might indicate the existence of molecular states. Hopefully our work will be useful to the future lattice study and the investigation of possible molecular states.

Acknowledgment

This project is supported by the National Natural Science Foundation of China under Grants No. 11075004, No. 11021092, No. 11035006, No. 11047606, No. 10805048, and the Ministry of Science and Technology of China (No. 2009CB825200), and the Ministry of Education of China (FANEDD under Grants No. 200924, DPFIHE under Grants No. 20090211120029, NCET under Grants No. NCET-10-0442, the Fundamental Research Funds for the Central Universities under Grants No. lzujbky-2010-69). YRL was partially supported by JSPS KAKENHI (21.09027).

References

1. C.-H. Lee, H. Jung, D.-P. Min, and M. Rho, Phys.Lett.B **326**, 14 (1994).
2. M. Mojzis, Eur.Phys.J.C **2**, 181 (1998).
3. N. Kaiser, Phys. Rev. C **64**, 045204 (2001).
4. T. D. Cohen and R. F. Lebed, Phys. Rev. D **74**, 056006 (2006).
5. G.-Z. Meng, *et al.*, Phys. Rev. D **80**, 034503 (2009).
6. D. Gamermann, E. Oset, D. Strottman, and M. J. V. Vacas, Phys. Rev. D **76**, 074016 (2007).

7. A. Torok, *et al.*, Phys. Rev. D **81**, 074506 (2010).
8. S. Scherer, Adv.Nucl.Phys. **27**, 277 (2003).
9. Y.-R. Liu, X. Liu, and S.-L. Zhu, Phys. Rev. D **79**, 094026 (2009).
10. F. Guo, C. Hanhart, and U. Meißner, Eur.Phys.J. A **40**, 171 (2009).
11. L. Geng, N. Kaiser, J. Martin-Camalich, and W. Weise, Phys.Rev.D **82**, 54022 (2010).
12. T.-M. Yan, *et al.*, Phys. Rev. D **46**, 1148 (1992).
13. P. Cho, Nucl.Phys.B **396**, 183 (1993).
14. M. B. Wise, Phys. Rev. D **45**, R2188 (1992).
15. R. Casalbuoni, *et al.*, Phys.Rep **281**, 145 (1997).
16. T. Becher and H. Leutwyler, Eur.Phys.J. C **9**, 643 (1999).
17. T. Becher and H. Leutwyler, JHEP **0106**, 017 (2001).
18. B. Kubis and U.-G. Meißner, Nucl.Phys.A **679**, 698 (2001).
19. S.-L. Zhu, S. Puglia, and M. J. Ramsey-Musolf, Phys. Rev. D **63**, 034002 (2001).
20. Z. Liu, Y. Liu, X. Liu, and S. Zhu, arXiv:1104.2726 (2011).
21. G. Ecker, J. Gasser, A. Pich, and E. D. Rafael, Nucl.Phys. B **321**, 311 (1989).
22. V. Bernard, N. Kaiser, and U.-G. Meißner, Phys.Lett.B **309**, 421 (1993).
23. L. Liu, H. Lin, and K. Orginos, arXiv:0810.5412 [hep-lat] (2008).
24. Y.-R. Liu and S.-L. Zhu, Phys.Rev.D **75**, 034003 (2007).